ACS OMEGA

Open Access

http://pubs.acs.org/journal/acsodf

Article

A Novel Approach for Nanosponge: Wool Waste as a Building Block for the Synthesis of Keratin-Based Nanosponge and Perspective Application in Wastewater Treatment

Gjylije Hoti, Fabrizio Caldera, Francesco Trotta, Marina Zoccola, Alessia Patrucco, and Anastasia Anceschi*

Cite This: *ACS Omega* 2024, 9, 43319−43330

Read Online

ACCESS | Metrics & More | Article Recommendations | Supporting Information

ABSTRACT: Wool waste is a huge environmental problem that needs to be addressed in order to avoid the continuous accumulation of biohazardous waste in landfills. In recent years, wool has proven to be an excellent source of keratin that can be used for various purposes. But never before has keratin from wool waste been used as a building block to synthesize a well-known class of biopolymers called nanosponges. Typically, nanosponges are produced by the reaction of cyclodextrins with an appropriate cross-linker to obtain an insoluble hyper-cross-linked polymer, which has applications in various fields. For this reason, a novel, affordable approach for the synthesis of a novel class of nanosponge using wool keratin as the building block has been presented. The keratin nanosponge was synthesized by reacting keratin with pyromellitic dianhydride as a cross-linking agent. The formation of a cross-linked polymer was successfully confirmed by CHNS-elemental analysis, TGA, DSC, FTIR-ATR, SEM, and water absorption capacity measurements. Surprisingly, the keratin-based nanosponge showed ∼50% uptake of heavy metals after only 24 h of contact time. The adsorption kinetics was also evaluated, indicating a pseudo-second-order model fit and the mechanism is predominantly the intraparticle diffusion process. The novel synthesized nanosponge proved to be a possible alternative for wastewater treatment.

INTRODUCTION

Natural fiber processing has the highest environmental impact, particularly wool.[1] Furthermore, water pollution caused by mainly anthropogenic activities is an extremely serious environmental problem that has emerged in recent years.[2] Thus, the time has come for a transition by proposing a new system with a vision aligned with the circular economy principle.

Industrial waste often contains a wide range of toxic dissolved inorganic chemicals that have been discharged into the environment, leading to severe water pollution. These pollutants include heavy metal ions, colorants, phenols, organic compounds, and inorganic ions.[3,4] Heavy metals have become increasingly prevalent in aquatic systems due to excessive discharges from various industries, such as metallurgical and chemical fertilizer production.[5,6] As a result, many aquatic environments now have metal concentrations in excess of water quality criteria, and there is a need to develop measures to protect ecosystems, fauna, and flora, as well as human health. Studies conducted during the past few years have shown that even low concentrations of heavy metals can cause acute lethal toxicity because of their ability to accumulate and nonbiodegradable nature.[7]

Based on that, the removal of heavy metals in water has attracted significant attention, and various methods have been applied. Various techniques are commonly used to treat heavy metal pollution in wastewater, including chemical precipitation,[8] membrane filtration,[9] electrochemical treatment,[10] solvent extraction,[11] ion exchange,[12] and adsorption.[13] Chemical precipitation and electrochemical treatment are commonly used, but they produce a large quantity of sludge that is difficult to be treated.[14] Membrane filtration, solvent extraction, and ion exchange are expensive and difficult to be applied at a large scale.[15] Thus, these techniques have some shortcomings, such as complex processing, being expensive, and being energy-consuming. An ideal alternative is considered adsorption. Adsorption is currently used for industrial applications and it is considered ideal for wastewater treatment because of its simplicity and cost-effectiveness.[16] Over the last

Received: November 16, 2023
Revised: September 2, 2024
Accepted: September 5, 2024
Published: October 16, 2024

few decades, various materials have been developed as adsorbents for heavy metal removal.[17] Numerous agriculture and industrial byproducts and wastes have been studied as low-cost adsorbents.[18,19] Recently, keratinous materials such as wool, feathers, and hair have been explored.[20−22] Among these, wool is relatively abundant and sheep production and wool processing generate a significant amount of unused materials that are generally landfilled or discarded, creating possible environmental problems.[23] Thus, scientists have increasingly become interested in using wool for many potential applications.[24] Specifically, wool found applications as a natural biosorbent because of its high ability to remove metals to trace concentrations.[25] Wool can bind a wide range of metal ions, but more effective metal removal is obtained with chemically modified wool fibers or extracted wool protein.[26] Recently, many researchers have explored the extraction of keratin from wool and its transformation into new materials for different applications, including films, cosmetics, medical membranes, injectable gel, and drug delivery systems.[27] Based on the application, different extraction approaches have been performed. Reducing agents or oxidants are often used to extract keratin, but also physicochemical methods such as hydrothermal or steam explosion techniques are commonly applied.[28−30] Various extraction methods lead to differences in recovery, morphology, and physicochemical properties of keratin, and in this paper, sulfitolysis has been applied for keratin extraction. It is known that keratin has the ability to bind toxic substances such as heavy metals and other hazardous VOCs, but the poor mechanical properties of wool keratin limit its processing and practical applications.[31] Therefore, keratin should be appropriately treated to achieve better structural properties and overcome the aforementioned problems.

One possible way is to explore the use of keratin as a building block for the synthesis of new biobased polymers, tailoring their chemical and physical properties.[32,33] Many cross-linking agents are available and well-established, such as epichlorohydrin, diacyl chlorides, dialdehydes, epoxides, etc. The cross-linking reaction is typically performed using cellulose or starch-based compounds in order to create a well-known class of insoluble polymers, known as nanosponge.[34] Many research studies report the use of different building blocks for the formation of nanosponges, but no previous work described the use of protein for the nanosponges synthesis.

This work presents the synthesis of a novel class of nanosponges using keratin as a building block. Specifically, the keratin was cross-linked using the pyromellitic dianhydride (PMDA) as a cross-linking agent, and the obtained nanosponge was fully characterized using TGA, IR, DSC, and SEM. In addition, the preliminary adsorption experiments of some metal cations (Pb, Cd, and Ni) from aqueous solutions were carried out to demonstrate the potential of the keratin-nanosponge (Ker-Ns) in wastewater treatments.

MATERIALS AND METHODS

2.1. Materials. Pyromellitic dianhydride (PMDA, 97%); dimethyl sulfoxide (DMSO, (≥99.9%); triethylamine (Et_3N, ≥ 99%); acetone (≥99% (GC)), sodium hydroxide (NaOH, 99%), urea (98%), and sodium metabisulfite (>99%) were purchased from Sigma-Aldrich (Darmstadt, Germany).

2.2. Methods. *Keratin Extraction.* Prior to extraction, coarse wool samples are in the form of tops. The fibers were cleaned using a Soxhlet extraction with petroleum ether to remove any grease and surfactants present on the wool surface. Then, 4 g of wool fibers was soaked in 100 mL of an aqueous solution containing urea (8 M) and sodium metabisulfite (0.5 M) and brought to pH 7 with NaOH (5 M). After that, the solution was shaken for 2.5 h at 65 °C using a Heraeus Linitest apparatus (URAI S.p.A., Assago, Italy). Then, the mixture underwent filtration using a 5 μm pore-size filter and was subsequently dialyzed with a cellulose dialysis tube (molecular weight cut off 12−14 kDa) against distilled water in a circulating system for 2 days. The resulting solution was then dried using a freeze-dryer for a week. The extraction yield was determined as described below:

$$Y(\%) = \frac{W_e}{W_w} \quad (1)$$

The yield Y *(%)* define the extraction yield and it is calculated using the formula 1) where W_e represents the dry weight of extracted keratoses achieved after lyophilization, and W_w is the initial weight of wool.

Synthesis of Keratin-Pyromellitic Dianhydride-Based Nanosponge (Ker-Ns). The nanosponge synthesis was carried out by dissolving 0.44 g of anhydrous extracted keratin in 3.58 mL of DMSO in a vial, following the procedure already described in the available literature without any modifications[35] A homogeneous and colorless mixture was prepared and 0.22 mL of Et3N was added as a catalyst, followed by the incorporation of 0.42 g of PMDA as cross-linking agent. Because of the exothermic character of the reaction, it was performed under a magnetic stirrer at room temperature. The entire polymerization process was completed within a few minutes, resulting in a solid that was left to set for 24 h. The solid mass was then manually ground in a mortar and repeatedly washed with deionized water using a Buchner filtration system until a clear supernatant solution was obtained. Any potential byproducts were completely removed in a Speed Extractor (BUCHI E-914) with acetone for about 40 min. Finally, the Ker-Ns was allowed to air-dry, ground, and used for characterization. The yield of the reaction is approximately 40%.

CHNS-Elemental Analysis. The CHNS-elemental analysis (EA) was performed to precisely and reproducibly quantify the carbon, hydrogen, nitrogen, and sulfur contents in the synthesized Ker-Ns. The analysis was conducted using a CHNS-O analyzer (Thermo Fisher Scientific FlashEA 1112 series; Waltham, MA, USA) equipped with Eager Xperience software (for Windows XP) and MAS 200R Auto Sampler. The external standard utilized for system calibration was 2,5-bis(5-*tert*-butyl-2-benzo-oxazol-2-yl) thiophene (BBOT). Specifically, the analysis was performed by employing a metal container that is filled with approximately 2.5 mg of sample and an equivalent quantity of V_2O_5 as a catalyst.

ATR Analysis. The attenuated total reflection (ATR) technique equipped with a Smart Endurance diamond crystal was used to collect the FTIR spectra of keratin and Ker-Ns. The spectra were gathered in the range of 4000 to 650 cm^{-1} with 64 scans and 4 cm^{-1} resolution using a Thermo Nicolet Nexus IZ10 spectrometer (Milan, Italy) with Omnic software.

Thermogravimetric Analysis. The TGA Mettler Toledo instrument (Columbus, Ohio-USA) with a STARe system was used to perform the thermogravimetric analyses under a nitrogen flow of 100 mL min^{-1}. About 10 mg of keratin and

https://doi.org/10.1021/acsomega.3c09133
ACS Omega 2024, 9, 43319−43330

Ker-Ns were placed in an alumina open pan and heated to 700 °C by a ramping temperature of 10 °C min^{-1}.

Differential Scanning Calorimetry Analysis. TA 3000 Mettler Toledo instrument (Columbus, Ohio-USA) with DSC 20 cell was utilized for the Differential Scanning Calorimetry analysis (DSC). The program operated in the interval of temperature of 30 to 220 °C with a heating rate of 10 °C min^{-1} under nitrogen flow (50 mL min^{-1}).

Scanning Electron Microscopy. The samples were morphologically investigated with a Zeiss EVO 10 SEM. The scanning electron microscope (SEM) was operated at an acceleration voltage of 30 V and a 50 pA probe. The samples were fixed on aluminum holders with double-sided adhesive tape. Later on, the samples were covered with 20−30 nm of gold in argon using an Emitech K 550 sputter coater with a 20-mA current for approximately 180 s.

Water Absorption Capacity (WAC). For assessing the water absorption capacity, 50 mg of dry powder was vortex-mixed with 1.5 mL of deionized water in an Eppendorf tube. The tube was then enclosed and kept under ambient conditions. After 2 h, the water-bound material was retrieved through the centrifugation step to isolate the unabsorbed water layer. After removal of the supernatant, we blot off any residual excess water using absorbent paper and record the weight. Calculate the water absorption capacity (%WAC) using eq 2:[35]

$$\text{WAC}\ (\%) = \frac{m_t - m_o}{m_o} \times 100 \tag{2}$$

The mass of the swollen sample at time t (m_t) and the initial weight of the dry sample (m_o) were measured.

Three replicates were executed to ensure accuracy.

ICP-OES Analysis. The quantification of Ni^{2+}, Pb^{2+}, and Cd^{2+} adsorption was performed using inductively coupled plasma-optical emission spectroscopy (ICP-OES) with a PerkinElmer Optima 7000 DV apparatus. The equipment was supplied with an Echelle monochromator, a cyclonic spray chamber, and a Teflon Mira Mist nebulizer. The plasma power was set to 1.3 kW, and the sample aspiration rate was set to approximately 2 mL min^{-1}. Regarding the nebulizer, the argon nebulizer flow was set to 0.6 L min^{-1}, while the argon auxiliary flow was set to 0.2 L min^{-1}, and the argon plasma flow was set to 15 L min^{-1}. The adsorption experiments began with 50 mL of a 50 ppb solution of Ni^{2+}, Pb^{2+}, and Cd^{2+}. The experiment involved immersing 2 mg of Ker-Ns in solutions at ambient temperature for different intervals spanning from 1 to 24 h. Prior to immersion, the solutions were passed through a 0.45 μm PTFE filter, and then 1% v/v nitric acid (65% w/v) was subsequently added. The concentration values were based on the average of three separate readings. The ICP-OES data are reported in μg mg^{-1} according to the eq 3:

$$C = \frac{V(C_0 - C_e)}{m} \tag{3}$$

where V is the volume of the tested solution (5 mL), C_0 is the starting concentration of the metal in the solution (expressed in mg L^{-1}), C_e is the concentration of the unadsorbed heavy metal (expressed in mg L^{-1}), and m is the amount of Ker-Ns (5 mg).

To evaluate the materials' regeneration capability, desorption experiments were conducted by adding the extracting solution to the wet samples. The process began with the application of a saline solution of 0.01 M KCl at a circumneutral pH, followed by a subsequent 0.1 M NaOH washing step. The suspensions were shaken for 24 h at 25 °C in the dark. No changes in content were made, and the text is free from bias and subjective evaluations.

Kinetic Studies. A kinetic study was performed to quantify the adsorption-rate-controlling steps in Ni^{2+}, Pb^{2+}, and Cd^{2+} uptake on Ker-Ns. The pseudo-first-order and pseudo-second-order kinetic models were applied for kinetic study. Specifically, the data were collected after different exposure times of the Ker-Ns with 50 μg L^{-1} Ni^{2+}, Pb^{2+}, and Cd^{2+} aqueous solutions. The metal concentration was analyzed by ICP-OES. The pseudo-first-order kinetic model is given with the following eq 4 as[36]

$$\log(q_e - q_t) = \log q_e - \left(\frac{k_1}{2.303}\right)t \tag{4}$$

where q_e and q_t, represent the amounts of metal ion adsorbed by Ker-Ns (mg g^{-1}) at steady-state and time, t, respectively. By slope of the linear plots of $\log(q_e - q_t)$ versus t, the pseudo-first-order rate constant, k_1 (min^{-1}) was evaluated.

Further, the pseudo-second-order kinetic model considered in this study is given with the following eq 5 as[36,37]

$$t/q_t = (1/h) + (1/q_e)t \tag{5}$$

where q_e and q_t are amounts of metal ions (mg g^{-1}) adsorbed by the Ker-Ns at equilibrium and at time t, *respectively. The initial rate of adsorption* h (mg/g min) was evaluated using the eq 6:

$$h = k_2 q_e^2 \tag{6}$$

The pseudo-second-order adsorption rate k_2 (g/mg min) was determined by t/q_t against the t linear plot.

Furthermore, the heavy metal adsorption mechanism was studied utilizing the interparticle diffusion model, which was strong-minded by using the eq 7.

$$q_t = k_{diff} t + C \tag{7}$$

where C is the intercept and k_{diff} is the intraparticle diffusion rate constant (mol $min^{-1/2}$ g^{-1}).

3. RESULTS AND DISCUSSION

Characterization of the Keratin-Based Nanosponge. After degreasing, the wool underwent sulfitolysis extraction to obtain keratin. Briefly, wool fibers were treated with an aqueous solution containing urea and sodium metabisulfite (0.5 M) in a Linitest apparatus for 2.5 h at 65 °C. The mixture was then filtered and dialyzed against deionized water for 2 days. The resulting solution was dried by using a freeze-drier apparatus and stored properly for future analysis and preparation. The extraction yield was approximately 33% (w/w). After extraction, the keratin was cross-linked with PMDA using Et_3N as a catalyst at room temperature (Figure 1). The cross-linking reaction involves the attack of the nonbonding nitrogen pair of electrons of Et_3N on the PMDA carbonyl group, forming an activated intermediate. This intermediate can react with hydroxyl, sulfhydryl, and amine groups of the keratin, releasing the catalyst back to the reaction medium.[38] Another anhydride can be formed within the same molecule of PMDA to continue the reaction, cross-linking the keratin molecules, since there is another available carboxylic group in the same molecule of PMDA.[39] PMDA is estimated to be the

https://doi.org/10.1021/acsomega.3c09133
ACS Omega 2024, 9, 43319−43330

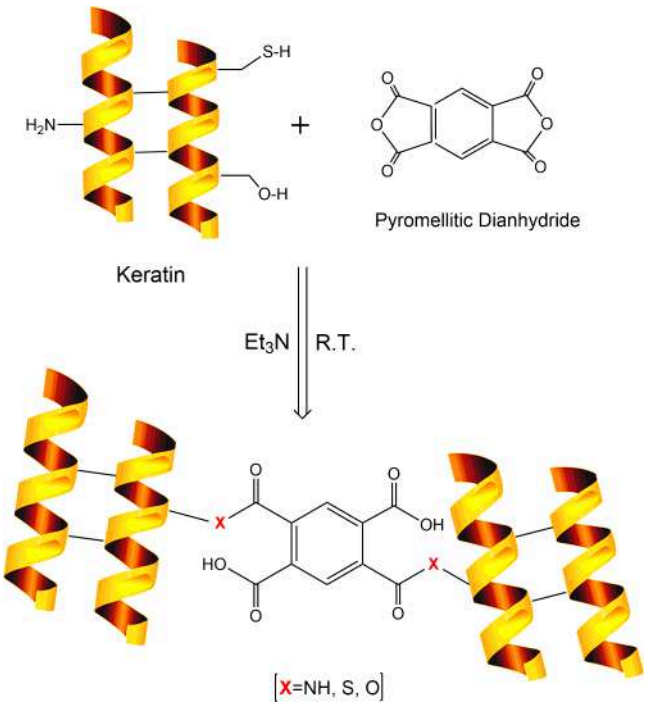

Figure 1. Cross-linking process of keratin with PMDA to form Ker-Ns.

most reactive dianhydride monomer due to the four carbonyl groups attached to one benzene ring in a coplanar conformation that may result in a high tendency to accept an electron. The PMDA-based ester-bridged polymeric network comprises free carboxylic acid groups, which enable the formation of complexes with both cations and apolar organic molecules.[35]

To get more insight into the cross-linking of keratin with PMDA, CHNS-elemental analysis was performed. The results are listed in Table 1.

Table 1. CHNS-Elemental Analysis of Keratin Sulfitolysis and Ker-Ns

samples	%N	%C	%H	%S
keratin sulfitolysis	13.08	41.96	6.51	5.88
keratin sulfitolysis/PMDA	12.62	46.17	6.15	4.28

The results show that the amount of carbon within the Ker-Ns structure is higher compared to the amount of carbon contained in bare keratin. This variation may be attributed to the presence of pyromellitic dianhydride, which led to an increase in the amount of carbon in the material. These results provide evidence that some modifications related to the cross-linking reaction have occurred.

After the CHNS-elemental analysis, ATR-FTIR spectroscopy was used to confirm the chemical structure of the developed Ker-Ns.

Figure 2a presents the FTIR spectra of keratin and Ker-Ns. Both spectra exhibit typical peaks corresponding predominantly to the peptide bonds in the amine A (3390−2800 cm^{-1}), amide I (1700−1600 cm^{-1}), amide II (1580−1480 cm^{-1}), and amide III (1300−1220 cm^{-1}) regions. The main vibrational modes are reported in Figure 2c.[40] No significant differences were observed in amide A, amide I, and amide II regions. However, Figure 2b displays modifications of functional groups detected in the amide III region. A new peak at 1365 cm^{-1} appears in the spectrum of cross-linked keratin, which is related to O−H bending of the carboxyl group. Additionally, a new strong absorption band of 1105 cm^{-1} is observed, which is attributed to C−O stretching. These new bands suggest that PMDA has been cross-linked to the keratin backbone through condensation reactions. The cross-linking reaction between the protein and the cross-linker may have involved acid and base groups of specific amino acid side chains, particularly amide linkages. These groups were not identified in the FTIR spectrum. However, the presence of two bands in Ker-Ns suggests a successful cross-linking reaction between keratin and PMDA. Further information about the FTIR analysis is reported in the Supporting Information, SI (Figure S1).

In order to investigate the morphology, SEM was used to characterize Ker-Ns at 50× and 500× magnifications, as shown in Figure 3.

After extraction, the keratin is typically subjected to a freeze-drying process to remove water and form a solid keratin powder. Figure 3a,b shows SEM micrographs of the keratin, revealing uniform amorphous keratin sheets. In contrast, Ker-NS displays a different morphology consisting of single particles with rough and jagged surfaces, as shown in Figure 3c,d. The particle size distribution ranges from 10 to 300 μm and is inhomogeneous due to the grinding process that occurred after the Ker-Ns synthesis.

To gain more insight, thermal analyses were used to characterize keratin and Ker-Ns. The TGA, DTGA, and DSC results are displayed in Figure 4.

The thermal profile of keratin, as shown by TGA (Figure 4a), exhibits two distinct weight loss steps, as highlighted by the DTGA analysis (Figure 4b). The first step, which represents evaporation/dehydration, begins immediately and concludes around 110 °C. This step accounts for a 10% weight loss and is dependent on the sample's moisture content. The second step, which occurs between 230 and 490 °C, corresponds to the degradation of the protein chain. For the Ker-Ns, three main weight loss steps are observed. The initial step begins promptly and concludes at approximately 110 °C and is associated with the loss of adsorbed moisture. Notably, the second degradation step occurs within the range of 180−240 °C and is evident in the DTGA. As keratin degradation typically occurs between 230 and 240 °C, as demonstrated by the TGA, the shift in the primary degradation peak raises the possibility of the presence of new bonds weaker than peptide bonds. After 240 °C, the keratin's main step of degradation can be observed between 240 and 350 °C. The split and shift of the Ker-Ns degradation step to a lower temperature indicates the presence of various types of bonds related to the cross-linking reaction.

Figure 4c shows the DSC analyses of keratin and Ker-Ns. To enhance the analysis, a pretreatment (not shown) was performed at a temperature of 100 °C to remove absorbed water. The Ker-Ns curve displays an additional endothermic peak at 180 °C, which may be attributed to the presence of −COOH or −OH groups. These groups primarily belong to PMDA, which is a poly(carboxylic acid). Not all of its functionalities are involved in cross-linking with keratin and as the temperature increases, these groups can condense and form a further cross-linked structure.[41] Further information on the

https://doi.org/10.1021/acsomega.3c09133
ACS Omega 2024, 9, 43319−43330

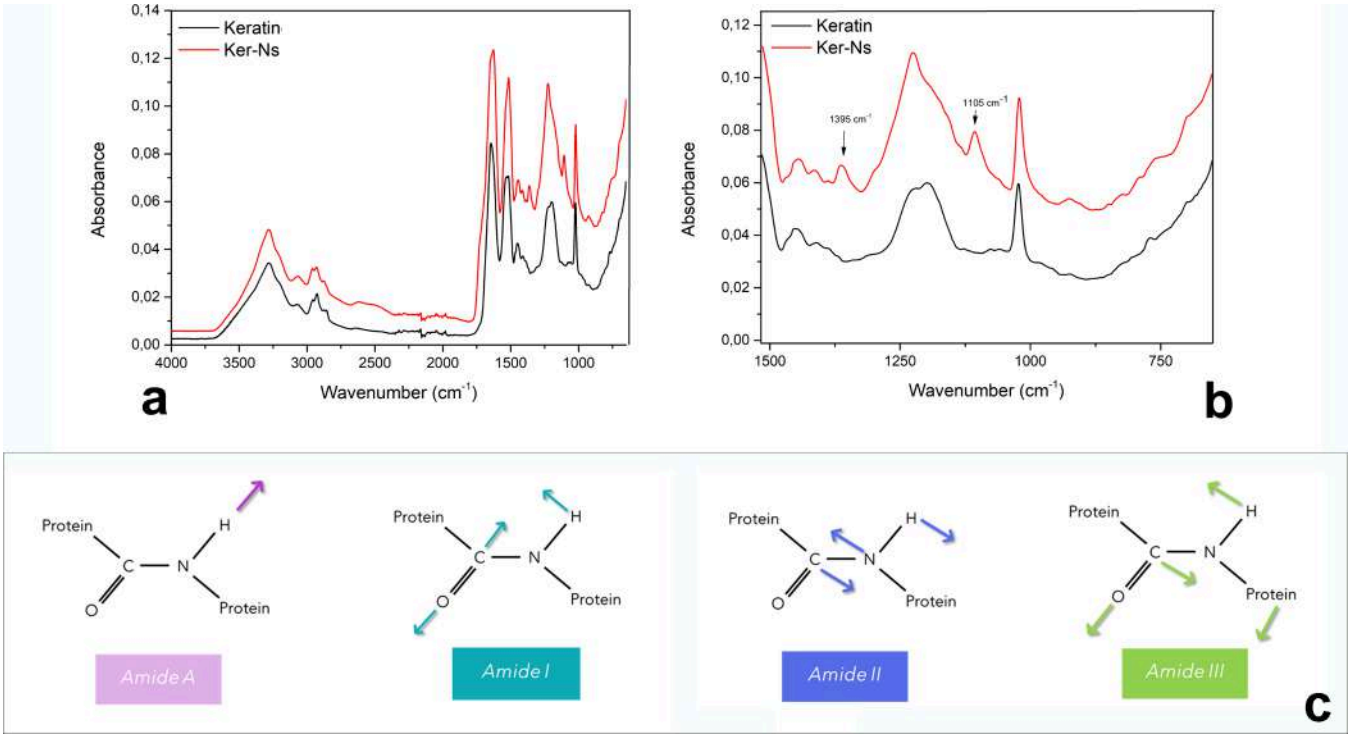

Figure 2. (a) FTIR spectra of keratin and Ker-Ns between 4000 and 650 cm^{-1}, (b) FTIR spectra of keratin and Ker-Ns between 1500 and 650 cm^{-1}, and (c) amine present in the keratin structure.

DSC analysis is reported in the Supporting Information (Figure S2).

Generally, a cross-linked polymer can increase its volume many times by absorbing large quantities of solvent. The swollen polymer network is held together by molecular chains that are chemically linked or so-called cross-links.[42] Therefore, swelling is essential for studying new materials' water-holding ability and permeability. Water molecules penetrate the network during swelling, causing the hydration of polar hydrophilic groups. Therefore, the polymer expands until equilibrium between the free water molecules and molecules within the network is achieved. The swelling index or obtained WAC is 245% (±5%) for the Ker-Ns, and 31% (±3%) for the bare keratin. The results indicate that the addition of the PMDA as a cross-linking agent has significantly tuned the hygroscopic behavior of the keratin, and thus, the Ker-Ns absorbed a higher quantity of water. Therefore, this higher swelling capability can be linked to the generation of a hydrophilic polymeric network created by the cross-linking reaction between the PMDA and keratin. This can induce the linkage of the water molecules through hydrogen bonds with hydrophilic groups. The WAC is substantial for diverse applications such as the removal of dyes and heavy metals from wastewater. Therefore, WAC is a notable step to further characterize the Ker-Ns as promising adsorbents in wastewater treatment.[43]

3.2. Metal Binding. The Ker-Ns contain many functional groups and therefore can have strong chelating ability with heavy metal ions. The effectiveness of Ker-Ns in removing heavy metals was assessed by immersing it in aqueous solutions of Ni^{2+}, Pb^{2+}, and Cd^{2+} and measuring the remaining ions in the solution using ICP-OES at various soaking times (1, 3, 5, and 24 h). The ICP-OES data were calculated and normalized to each sample weight, and the results are shown in Figure 5a. Furthermore, Table S1 in the Supporting Information provides a detailed overview of the adsorption capacity of keratin-based nanosponges (Ker-Ns) for nickel (Ni), cadmium (Cd), and lead (Pb) from aqueous solutions.

As shown in Figure 5a, the Ker-Ns gradually adsorb Cd^{2+}, Ni^{2+}, and Pb^{2+}. The Ker-Ns showed a rapid increase of metal ions adsorption in the first 3 h and after that, the adsorption rate sharply decreased and the adsorption reached the equilibrium in about 24 h. An increase of contact time up to 24 h resulted in only 1% adsorption over those obtained for 5 h of contact time, thus it can be noted that the maximum adsorption capacity has been reached. Indeed, the filling up of the Ker-Ns reactive site significantly affects the enhancement in adsorption after 24 h. After 24 h of adsorption, a high capacity for metal ion adsorption was achieved.

The maximum adsorption for Cd^{2+} was 56%, while those for Pb^{2+} and Ni^{2+} were 55 and 54%, respectively. These results are comparable to or better than those reported in alternative research on new types of adsorbents, considering that the values obtained are related to an initial concentration of metal ions of 50 ppb. A relatively low concentration was selected in reference to testing the adsorption capabilities of Ker-Ns in critical environments for metal ion complex formation. Typically, metal ion levels in effluent streams are on the order of parts per billion (ppb). In addition, according to the data found in the literature, these selected conditions allow the evaluation of the efficiency of wastewater treatment per gram of adsorbent.[44] Finally, desorption experiments were conducted on samples saturated with heavy metals to assess the potential for regenerating exhausted sorbents. The Ker-NS was washed with two different solutions, 0.01 M KCl and 0.1 M NaOH. As shown in Figure 5b, less than 1% of adsorbed Pb^{2+}, Cd^{2+}, and Ni^{2+} could not be fully removed, indicating the feasibility of recycling the Ker-NS.

https://doi.org/10.1021/acsomega.3c09133
ACS Omega 2024, 9, 43319−43330

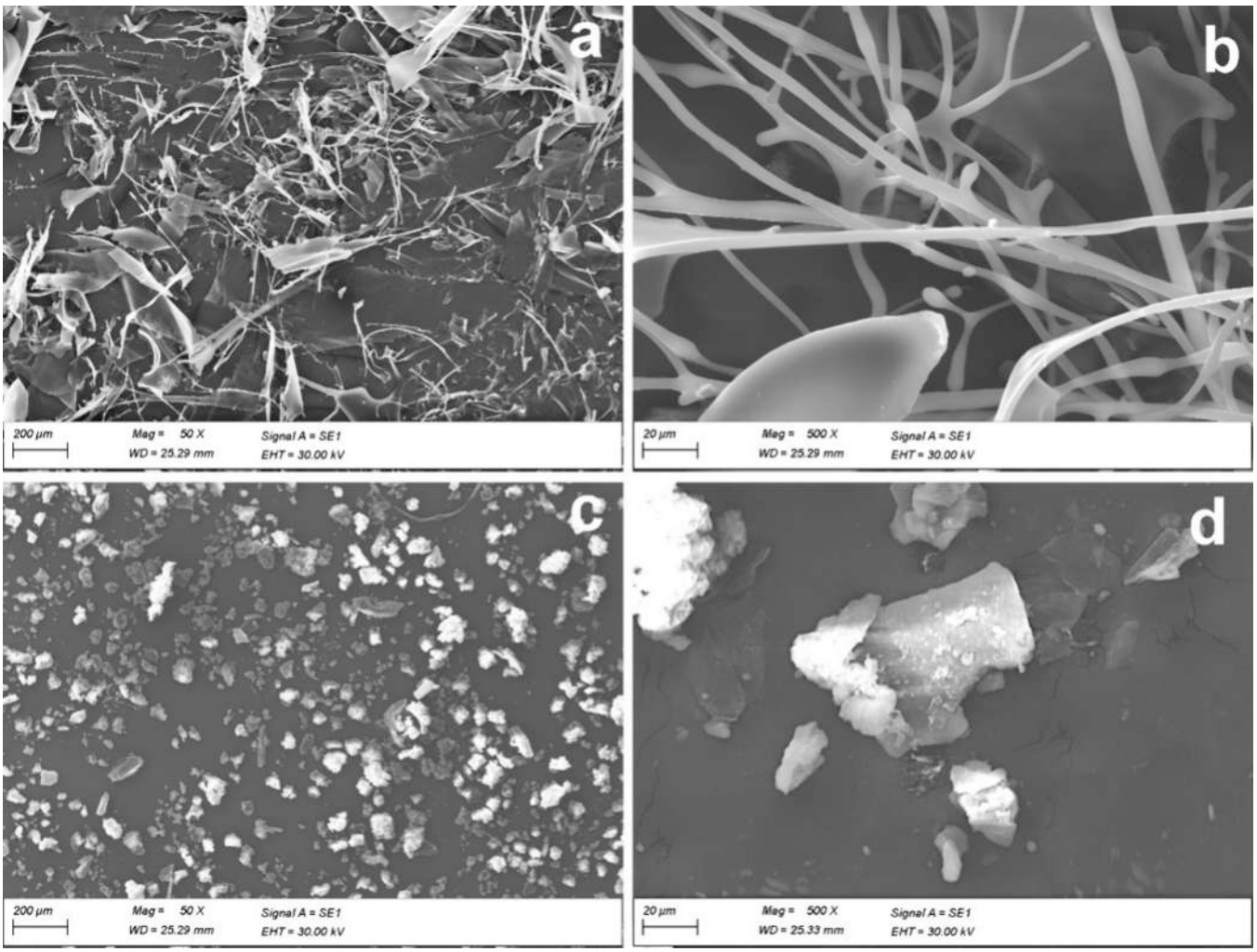

Figure 3. SEM micrographs of (a) keratin at 50×; (b) keratin at 500×; (c) Ker-Ns at 50×; (d) Ker-Ns at 500×.

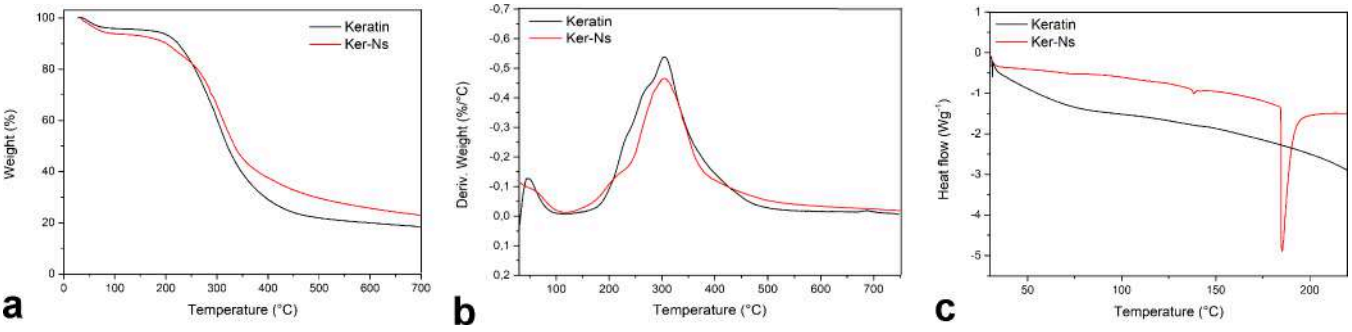

Figure 4. (a) TGA, (b) DTGA, and (c) DSC of Keratin (black line) and KER-Ns (red line).

The effective metal binding capacity of Ker-NS highlights its potential as a viable material for wastewater treatment and environmental remediation. Its ability to selectively adsorb heavy metals from aqueous solutions positions it as a sustainable alternative to traditional adsorbents, which often suffer from higher costs and environmental impact.

Since the Ker-Ns prove to be effective in heavy metal adsorption, the kinetic parameters associated with Cd^{2+}, Pb^{2+}, and Ni^{2+} removal have been studied. The kinetic parameter study provides further information about the adsorption process and the heavy metal uptake rate. This enables additional data for future applications in wastewater treatments. Consequently, the adsorption mechanism of Cd^{2+}, Ni^{2+}, and Pb^{2+} has been evaluated, fitting the adsorption data with the pseudo-first-order and pseudo-second-order models. For the pseudo-first-order, the adsorption results were evaluated by using eq 4, whereas for the pseudo-second-order, the adsorption results are shown in eqs 5 and 6. The plots obtained for Cd^{2+}, Pb^{2+}, and Ni^{2+} are presented in Figure 6.

The pseudo-first-order kinetic model (Figure 6a) is generally used to describe the physisorption processes, where the rate of adsorption is directly proportional to the number of available active sites. In contrast, the pseudo-second-order model (Figure 6b) is typically employed to elucidate the mechanisms

https://doi.org/10.1021/acsomega.3c09133
ACS Omega 2024, 9, 43319−43330

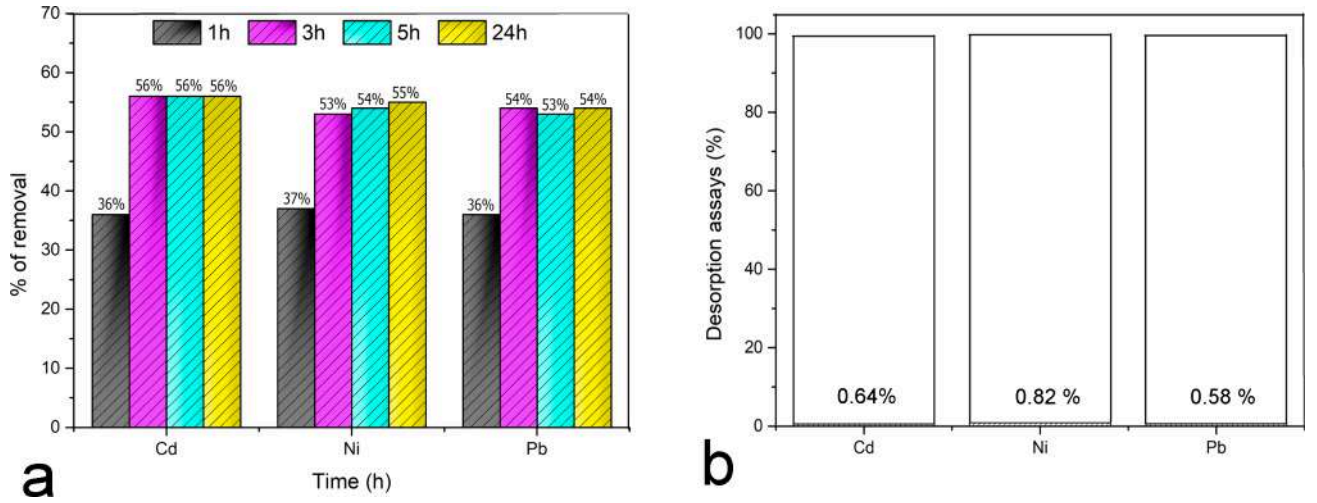

Figure 5. Percentage of (a) heavy metals removed by Ker-Ns vs contact time (h); (b) heavy metals not removed after washing.

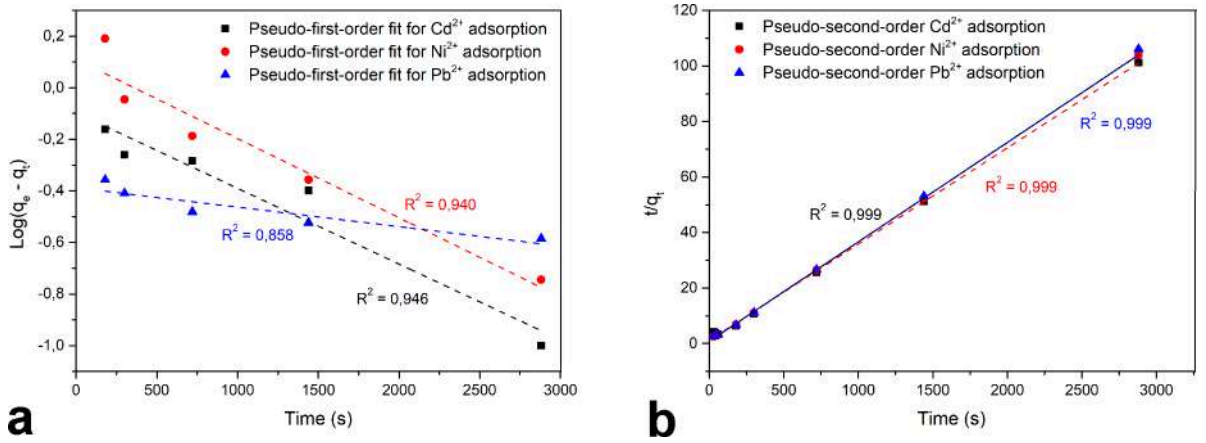

Figure 6. (a) Pseudo-first-order and (b) pseudo-second-order plots for Ker-Ns for Pb, Cd, and Ni adsorption.

Table 2. Kinetic Parameters for the Adsorption of Cd, Ni, and Pb on Ker-Ns

heavy metal	pseudo-first-order				pseudo-second-order			
	R^2	k_1 (min^{-1})	q_{eexp}(mg/mg)	q_{ecalc}(mg/mg)	R^2	k_2(mg/mg min)	q_{eexp}(mg/mg)	q_{ecalc}(mg/mg)
Cd^{2+}	0.945	-3.0×10^{-3}	28.55	0.41	0.999	0.035	28.55	28.01
Ni^{2+}	0.934	-3.0×10^{-3}	27.87	0.41	0.999	0.036	27.87	27.73
Pb^{2+}	0.858	-8.0×10^{-5}	27.45	0.28	0.999	0.037	27.41	27.11

intraparticle diffusion			
heavy metal	k_{diff} [$\mu g\ s^{-1/2}\ mL^{-1}$]	C	R^2
Cd^{2+}	0.014	27.67	0.984
Ni^{2+}	0.021	26.57	0.981
Pb^{2+}	0.0037	26.96	0.975

underlying the chemisorption processes. From the pseudo-first-order and pseudo-second-order models, the corresponding constant values k_1 and k_2, respectively, have been calculated from the slope of the linear fittings. Additionally, the goodness of fit was ensured by the value of the correlation coefficient R^2. Furthermore, the theoretical value $q_{ecalc}$was calculated for each kinetic model. All data obtained for Cd^{2+}, Ni^{2+}, and Pb^{2+} adsorption plots are listed in Table 2.

The correlation coefficient (R^2) for the pseudo-second-order is higher for all of the tested heavy metals than the one obtained from the pseudo-first-order plots. Particularly, R^2 for the Pb^{2+} is lower than the ones obtained for the Cd^{2+} and the Ni^{2+}, indicating a poor pseudo-first-order fitting of the Pb^{2+} experimental data. Furthermore, comparing the values q_{eexp} and q_{ecalc}, a wide difference between experimental and theoretical data is observed, suggesting that the pseudo-first-order model is not reliable for heavy metal adsorption into the Ker-Ns. In the pseudo-second-order case, the experimental and calculated q_e shows a good alignment with the experimental data. The R^2 for Cd^{2+}, Ni^{2+}, and Pb^{2+} are around 0.999, indicating that the pseudo-second-order kinetic is the suitable model to describe the adsorption mechanism of heavy metals into the Ker-Ns. The comparable values of Cd^{2+}, Ni^{2+}, and Pb^{2+} constant rate k_2 and q_e suggest that the adsorption mechanism followed by the

https://doi.org/10.1021/acsomega.3c09133
ACS Omega 2024, 9, 43319−43330

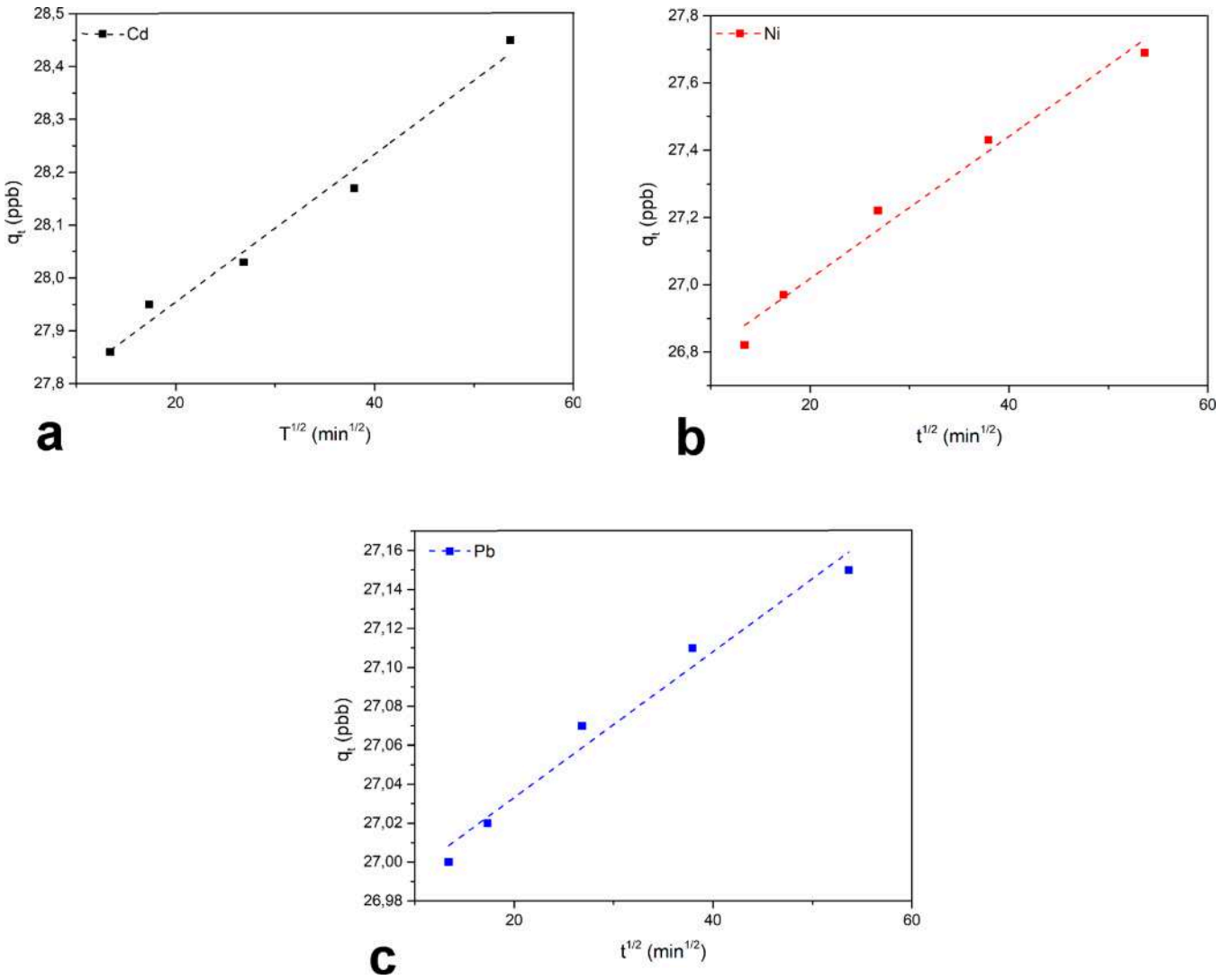

Figure 7. Intraparticles diffusion plots for (a) Cd^{2+}; (b) Ni^{2+}, and (c) Pb^{2+}.

tested heavy metals into the Ker-Ns match the results obtained in the adsorption mechanism of keratin fibers.[37] In conclusion, the pseudo-first-order model did not prove to be an accurate representation of the experimental data, suggesting that the adsorption process may not be primarily governed by physical adsorption or simple surface adsorption. In contrast, the pseudo-second-order model provided an excellent fit to the experimental data, and the value obtained for the adsorption capacities lends support to the hypothesis that chemisorption is the dominant mechanism. This suggests that chemical interactions, potentially involving covalent bonding or ion exchange, are crucial aspects of the adsorption process.

The adsorption phenomenon was also investigated. The adsorption generally consists of multiple-step mechanisms in which the solute moves from the bulk solution to the surface of the adsorbent. Then, it diffuses through the barrier layer and interacts with the active sites of the adsorbent, contributing to intraparticle diffusion. The study investigated the adsorption mechanism of Pb^{2+}, Cd^{2+}, and Ni^{2+} using the intraparticle diffusion model described in eq 7. The results are presented in Table 2 and illustrated in Figure 7 for Cd (Figure 7a), Ni (Figure 7b), and Pb (Figure 7c).

Interestingly, the value of q_t has been found for all of the analyzed heavy metals to be linearly correlated with the values of $t^{1/2}$. As regards the Cd, the k_{diff} value is about 0,014 $\mu g\ s^{-1/2}\ mL^{-1}$, whereas for Ni and Pb, the values were found to be 0.021 and 0.0037 $\mu g\ s^{-1/2}\ mL^{-1}$, respectively. The correlation coefficient is found to be high for all the investigated heavy metals, suggesting a satisfactory applicability of this model to characterize the adsorption mechanism. Additionally, the high C value suggests that intraparticle diffusion is the rate-determining step, as it gives an estimation of the thickness of the interfacial layer.[45]

Practical Implication of Adsorption Results. The high R^2 values observed for the pseudo-second-order model, coupled with the evidence of intraparticle diffusion, suggest the presence of a complex adsorption mechanism involving multiple steps. Initially, metal ions may be rapidly adsorbed onto the external surface of Ker-NS, followed by slower diffusion into the porous network, where stronger chemical interactions occur. This finding has potential practical applications, as the kinetic analysis confirms the efficiency and potential of Ker-NS for heavy metal removal. By understanding the dynamics of adsorption, it is possible to optimize operational parameters, improve efficiency, and

https://doi.org/10.1021/acsomega.3c09133
ACS Omega 2024, 9, 43319−43330

design systems that maximize the benefits of using Ker-NS for heavy metal removal. In particular, the kinetic study indicates that the adsorption process reaches equilibrium within 24 h, with most of the metal ions being adsorbed within the first few hours. This information is crucial for designing treatment systems where the contact time can be adjusted to ensure maximum efficiency. Shorter contact times can lead to reduced operational costs and higher throughput in continuous flow systems. Furthermore, understanding the rate of adsorption helps in selecting the appropriate reactor design. For example, a fixed-bed column might be suitable for applications requiring rapid adsorption, whereas batch reactors could be used for systems in which longer contact times are feasible. In addition, the ability to regenerate Ker-NS after saturation is a critical factor for its practical application. The kinetic results can inform the development of regeneration protocols, such as chemical desorption or thermal treatment, to restore the capacity of the adsorbent. An efficient regeneration can significantly reduce operating costs and waste generation, reducing the overall environmental footprint of the treatment process. Nevertheless, the effective removal of heavy metals to trace concentrations helps industries meet stringent regulatory standards for effluent discharge. This compliance is crucial for maintaining environmental quality and avoiding penalties or shutdowns.

Comparison with Commercial Adsorbent Materials Used for Metal Removal. Heavy metal ions are commonly removed from wastewater using adsorption techniques due to their low operating costs and high removal capacity.[15] Various types of porous materials have been developed for wastewater remediation including carbon materials such as activated carbons, carbon nanotubes, and graphene. These materials are widely used for heavy metal removal due to their large surface area (500−1500 m^2/g).[46] The ability of these materials to adsorb heavy metals varies from 89 mg/g to 890 mg/g depending on the type of carbonaceous material or activation process.[47] Another commonly used material for the adsorption of heavy metals is chitosan-based adsorbents. Chitosan is a natural polymer with a high affinity toward pollutants in wastewater.[48] However, it has a low mechanical strength and poor stability. To overcome these drawbacks, structural and chemical modifications have been proposed, such as chemical modification, composite synthesis, or grafting actions. These modifications can alter the selectivity and uptake of heavy metals, resulting in significant variations in heavy metal adsorption. For example, the adsorption of Pb^{2+} typically ranges from 13 mg/g to 1385 mg/g, while for Ni^{2+} it ranges from 68 mg/g to 254 mg/g, and for Cd^{2+} it ranges from 27 mg/g to 178 mg/g.[49] Other adsorbents considered good candidates for water purification with low operating costs are mineral adsorbents such as zeolite, silica, and clays.[50] According to the literature, natural zeolites have a typical range of cation exchange capacity of 2−4 mequiv per gram, while modified zeolites have an adsorption range of 96 to 100% for Ni^{2+}, Pb^{2+}, and Cd^{2+}, depending on the initial concentration value.[51] Another promising category of adsorbent materials is magnetic adsorbents. Magnetic adsorbents are a type of material where the matrix contains iron particles, typically magnetic nanoparticles like Fe_3O_4.[52] Various materials can be utilized as building blocks for the synthesis of magnetic matrices, including carbon materials, polymers, starch, or biomass. The adsorption capacity varies depending on the type of magnetic material used and the adsorption conditions.[53]

The most relevant research on heavy metal adsorption materials is related to the use of biobased adsorbents. Several new biopolymers or organic-based materials have been developed for this purpose. One of the most promising categories of biobased materials are metal−organic frameworks (MOFs). MOFs are generally synthesized by network synthesis, in which metal ions form bonds with organic linkers. Researchers have proposed thousands of MOFs, many of which have shown good ability in removing heavy metals. However, some of them have demonstrated poor stability in water.[15] Another interesting category of biobased materials is cyclodextrin-based nanosponges, which are capable of binding a large variety of metal ions. For example, cyclodextrin-based polymers in the form of fibers have shown an excellent response to heavy metals such as Cd^{2+} and Cu^{2+}, with a maximum adsorption capacity of 48.15 mg/g.[19] In a separate study, the nanosponge was synthesized through a reaction with pyromellitic dianhydride. It was found that at a concentration of 500 ppm of metal ions, the pyromellitic nanosponges had a retention capability higher than that of the citrate-based nanosponges. The pyromellitic nanosponges exhibited an adsorption capacity of 272 mg/g and 81 mg/g for Pb^{2+} and Cu^{2+}, respectively.[54]

Comparison with Other Keratin-Based Materials Used for Metal Removal. Protein-derived biomaterials have gained attention from researchers due to their versatile applications in various products. Keratin, in particular, is a convenient alternative because of its biodegradable and biodegradability properties.[55] Currently, scientists have successfully modified keratin for use as a bioremediation without a significant advance in the development of renewable materials.[56,57] Several materials have been used as sources of keratin for heavy metal removal. Table 3 provides an overview of some potential work done with keratin for comparison with the results obtained for Ker-Ns.

Table 3. Adsorption Capacity and Kinetic Order of Some Keratin-Based Materials

absorbent	studied metal ion	adsorption capacity(mg/g)	kinetic order	references
chicken feathers	Pb^{2+}	8.31	pseudo-second-order	58
chicken feathers	Zn^{2+}	4.31	pseudo-second-order	59
modified chicken feathers	Cr^{3+}	14.47		60
modified chicken feathers	As^{3+}	0.14	pseudo-second-order	61
eggshell membrane	Pb^{2+}	32.47	pseudo-second-order	62
eggshell membrane	Cd^{2+}	23.70	pseudo-second-order	62
wool	Pb^{2+}	43.30		63
horn hoof	Cu^{2+}	5.3	Pseudo-second-order	64

Furthermore, in a recent study chicken feathers keratin was modified in order to synthesize biopolymers named SM-03, SM-01, and SM-06. They found out that any modifications can decrease the adsorption of certain ions due to some physical and chemical modification of the structures.[65] Nevertheless, Zubair and co-workers tailored the adsorption properties of the

https://doi.org/10.1021/acsomega.3c09133
ACS Omega 2024, 9, 43319−43330

keratin by cross-linking it with nanochitosan particles.[66] The resulting keratin-derived biosorbents were fully characterized and used as biosorbent material. The sorption capacity of biosorbents was tested for eight different metals at different contact times, and the results underline that this new biosorbent is able to adsorb more than 98% of the initial metal concentration after a contact time of 24 h. Another interesting research paper proposes the use of dialdehyde cellulose nanocrystal and wool keratin, to remove Cd^{2+} from water media.[67] The prepared adsorbing material exhibited outstanding reusability, and the maximum adsorption efficiency was found to be 695.5 mg/g for Cd^{2+}, having a high exploitation potential for the purification of wastewater and effluents.

Considering the proposed materials for removing heavy metals, Ker-Ns fall into the category of new, efficient, and natural materials that can replace current wastewater treatment methods. The obtained data show that Ker-NS has properties comparable to those reported in the literature. The Ker-Ns show promising results in adsorbing heavy metals while maintaining high stability in water environments. The kinetic calculations support the potential applicability of this material in wastewater treatment. Additionally, it is economically and environmentally valuable, as it can be prepared from waste materials.

4. CONCLUSIONS

In the framework of circular economy, the wool waste keratin can be transformed into a high-added value material. Indeed, a novel biosorbent was prepared by cross-linking the wool keratin with the PMDA. The explored synthetic methodology possesses advantages, including a biocompatible and biodegradable product with a high yield and simple and safe reaction conditions. The successful formation of a novel polymer was further confirmed via FTIR, TGA, DSC, and SEM results. Moreover, the presence of free functional groups in the polymer network can be exploited for water remediation. The WAC for Ker-Ns is 245%, whereas that for the bare keratin is 31%. Ker-Ns can be considered an excellent adsorbent for the removal of $Cd^{2+,}$ Pb^{2+}, and Ni^{2+} in an aqueous solution. The efficacy of Ker-Ns as an adsorbent is investigated by varying contact time and analyzed using ICP-OES. Furthermore, the Ker-Ns showed ∼50% Cd^{2+}, Pb^{2+}, and Ni^{2+} removal after 24 h. Adsorption kinetics is determined using pseudo-first and pseudo-second-kinetic models. It is observed that the pseudo-second-kinetic models described the kinetic data for the heavy metal adsorption more accurately. These results lay the foundations for the use of wool waste in open-loop recycling, in which it is transformed into a novel biosorbent capable of removing heavy metals in water. This will empower the researchers to help solve ongoing environmental problems of water pollution sourced by heavy metal discharges. In addition, this investigation is essential to research for tailoring novel nanocarrier systems with excellent WAC and with the prospect of increasing their exploitation in countless industrial applications.

■ ASSOCIATED CONTENT

Supporting Information

The Supporting Information is available free of charge at https://pubs.acs.org/doi/10.1021/acsomega.3c09133.

Additional FTIR analysis (Figure S1); detailed differential scanning calorimetry (DSC) analysis (Figure S2); and adsorption capacity of keratin-based nanosponge for nickel (Ni), cadmium (Cd), and lead (Pb) (Table S1) (PDF)

■ AUTHOR INFORMATION

Corresponding Author

Anastasia Anceschi − *CNR-STIIMA, Italian National Research Council, Institute of Intelligent Industrial Technologies and Systems for Advanced Manufacturing, 13900 Biella, BI, Italy;* orcid.org/0000-0003-4234-0663; Email: anastasia.anceschi@stiima.cnr.it

Authors

Gjylije Hoti − *Department of Chemistry, University of Turin, 10125 Turin, Italy; Department of Drug Science and Technology, University of Turin, 10125 Turin, Italy*

Fabrizio Caldera − *Department of Chemistry, University of Turin, 10125 Turin, Italy*

Francesco Trotta − *Department of Chemistry, University of Turin, 10125 Turin, Italy*

Marina Zoccola − *CNR-STIIMA, Italian National Research Council, Institute of Intelligent Industrial Technologies and Systems for Advanced Manufacturing, 13900 Biella, BI, Italy;* orcid.org/0000-0002-5356-4817

Alessia Patrucco − *CNR-STIIMA, Italian National Research Council, Institute of Intelligent Industrial Technologies and Systems for Advanced Manufacturing, 13900 Biella, BI, Italy;* orcid.org/0000-0002-6105-0226

Complete contact information is available at: https://pubs.acs.org/10.1021/acsomega.3c09133

Notes

The authors declare no competing financial interest.

■ ACKNOWLEDGMENTS

Authors acknowledge support from Project CH4.0 under the MUR program "Dipartimenti di Eccellenza 2023-2027" (CUP: D13C22003520001).

■ REFERENCES

(1) Šajn, N. Environmental Impact of the Textile and Clothing Industry. What Consumers Need to Know. *Eur. Parliam. Res. Serv.* **2019**,. No. January

(2) Banat, F.; Al-Asheh, S.; Al-Rousan, D. Comparison between Different Keratin-Composed Biosorbents for the Removal of Heavy Metal Ions from Aqueous Solutions. *Adsorpt. Sci. Technol.* **2002**, *20* (4), 393−416.

(3) Muralikrishna, I. V; Manickam, V. Chapter Thirteen - Industrial Wastewater Treatment Technologies, Recycling, and Reuse; Muralikrishna, I. V; Manickam, V. B. T.-E. M., Eds.; Butterworth-Heinemann, 2017; pp 295−336. .

(4) Ahmed, J.; Thakur, A.; Goyal, A. *And Its Toxic Effects*. 2022, No. *5*, 1−14.

(5) Rajapaksha, A. U.; Alam, M. S.; Chen, N.; Alessi, D. S.; Igalavithana, A. D.; Tsang, D. C. W.; Ok, Y. S. Removal of Hexavalent Chromium in Aqueous Solutions Using Biochar: Chemical and Spectroscopic Investigations. *Sci. Total Environ.* **2018**, *625*, 1567−1573.

(6) Mondal, N. K.; Basu, S. Potentiality of Waste Human Hair towards Removal of Chromium(VI) from Solution: Kinetic and Equilibrium Studies. *Appl. Water Sci.* **2019**, *9* (3), 1−8.

(7) Mitra, S.; Chakraborty, A. J.; Tareq, A. M.; Emran, T. Bin; Nainu, F.; Khusro, A.; Idris, A. M.; Khandaker, M. U.; Osman, H.; Alhumaydhi, F. A.; Simal-Gandara, J. Impact of Heavy Metals on the Environment and Human Health: Novel Therapeutic Insights to Counter the Toxicity. *J. King Saud Univ. - Sci.* **2022**, *34* (3), No. 101865.
(8) Pohl, A. Removal of Heavy Metal Ions from Water and Wastewaters by Sulfur-Containing Precipitation Agents. *Water, Air, Soil Pollut.* **2020**, *231* (10), 503.
(9) Hube, S.; Eskafi, M.; Hrafnkelsdóttir, K. F.; Bjarnadóttir, B.; Bjarnadóttir, M. Á.; Axelsdóttir, S.; Wu, B. Direct Membrane Filtration for Wastewater Treatment and Resource Recovery: A Review. *Sci. Total Environ.* **2020**, *710*, No. 136375.
(10) Chen, G. Electrochemical Technologies in Wastewater Treatment. *Sep. Purif. Technol.* **2004**, *38* (1), 11−41.
(11) Chang, S. H. Utilization of Green Organic Solvents in Solvent Extraction and Liquid Membrane for Sustainable Wastewater Treatment and Resource Recovery—a Review. *Environ. Sci. Pollut. Res.* **2020**, *27* (26), 32371−32388.
(12) Gregory, J.; Dhond, R. V. Wastewater Treatment by Ion Exchange. *Water Res.* **1972**, *6* (6), 681−694.
(13) De Gisi, S.; Lofrano, G.; Grassi, M.; Notarnicola, M. Characteristics and Adsorption Capacities of Low-Cost Sorbents for Wastewater Treatment: A Review. *Sustain. Mater. Technol.* **2016**, *9*, 10−40.
(14) Janin, A.; Zaviska, F.; Drogui, P.; Blais, J.-F.; Mercier, G. Selective Recovery of Metals in Leachate from Chromated Copper Arsenate Treated Wastes Using Electrochemical Technology and Chemical Precipitation. *Hydrometallurgy* **2009**, *96* (4), 318−326.
(15) Qasem, N. A. A.; Mohammed, R. H.; Lawal, D. U. Removal of Heavy Metal Ions from Wastewater: A Comprehensive and Critical Review. *npj Clean Water* **2021**, *4* (1), 36.
(16) Arora, R. Adsorption of Heavy Metals-a Review. *Mater. Today Proc.* **2019**, *18* (1), 4745−4750.
(17) Hussain, A. *Removal of Heavy Metals from Wastewater by Adsorption*; Madan, S., Ed.; IntechOpen: Rijeka, 2021; . p Ch. 10.
(18) Anceschi, A.; Guerretta, F.; Magnacca, G.; Zanetti, M.; Benzi, P.; Trotta, F.; Caldera, F.; Nisticò, R. Sustainable N-Containing Biochars Obtained at Low Temperatures as Sorbing Materials for Environmental Application: Municipal Biowaste-Derived Substances and Nanosponges Case Studies. *J. Anal. Appl. Pyrolysis* **2018**, *134* (July), 606−613.
(19) Anceschi, A.; Caldera, F.; Bertasa, M.; Cecone, C.; Trotta, F.; Bracco, P.; Zanetti, M.; Malandrino, M.; Mallon, P. E.; Scalarone, D. New Poly(β-Cyclodextrin)/Poly(Vinyl Alcohol) Electrospun Sub-Micrometric Fibers and Their Potential Application for Wastewater Treatments. *Nanomaterials* **2020**, *10* (3), 1−15.
(20) Goyal, S.; Dotter, M.; Diestelhorst, E.; Storck, J. L.; Ehrmann, A.; Mahltig, B. Extraction of Keratin from Wool and Its Use as Biopolymer in Film Formation and in Electrospinning for Composite Material Processing. *J. Eng. Fiber. Fabr.* **2022**, *17*, 15589250221090500.
(21) Isarankura Na Ayutthaya, S.; Tanpichai, S.; Wootthikanokkhan, J. Keratin Extracted from Chicken Feather Waste: Extraction, Preparation, and Structural Characterization of the Keratin and Keratin/Biopolymer Films and Electrospuns. *J. Polym. Environ.* **2015**, *23*, 506.
(22) Cassoni, A. C.; Freixo, R.; Pintado, A. I. E.; Amorim, M.; Pereira, C. D.; Madureira, A. R.; Pintado, M. M. E. Novel Eco-Friendly Method to Extract Keratin from Hair. *ACS Sustain. Chem. Eng.* **2018**, *6* (9), 12268−12274.
(23) Zheljazkov, V. D. Assessment of Wool Waste and Hair Waste as Soil Amendment and Nutrient Source. *J. Environ. Qual.* **2005**, *34* (6), 2310−2317.
(24) Erdogan, U. H.; Seki, Y.; Selli, F. 9 - Wool Fibres. In *Woodhead Publishing Series in Textiles*; Kozłowski, R. M.; Mackiewicz-Talarczyk, M. B. T.-H. of N. F. (Second E., Eds.; Woodhead Publishing, 2020; pp 257−278. .
(25) Simonič, M.; Fras Zemljič, L. Functionalized Wool as an Efficient and Sustainable Adsorbent for Removal of Zn(II) from an Aqueous Solution. *Mater. (Basel, Switzerland)* **2020**, *13* (14), 3208.
(26) Abdolahpour, S.; Farrokhnia, A.; Abbasi, Z. Removal of Pb (Ii) Ion and Safranin Dye from Aqueous Solution by Sheep Wool. *Iran. J. Chem. Chem. Eng.* **2019**, *38* (5), 155−163.
(27) Lazarus, B. S.; Chadha, C.; Velasco-Hogan, A.; Barbosa, J. D. V; Jasiuk, I.; Meyers, M. A. Engineering with Keratin: A Functional Material and a Source of Bioinspiration. *iScience* **2021**, *24* (8), No. 102798.
(28) Du, W.; Zhang, L.; Zhang, C.; Cao, J.; Wang, D.; Li, H.; Li, W.; Zeng, J. Green and Highly Efficient Wool Keratin Extraction by Microwave Induction Method. *Front. Mater.* **2022**, *8*. .
(29) Tonin, C.; Zoccola, M.; Aluigi, A.; Varesano, A.; Montarsolo, A.; Vineis, C.; Zimbardi, F. Study on the Conversion of Wool Keratin by Steam Explosion. *Biomacromolecules* **2006**, *7* (12), 3499−3504.
(30) Bhavsar, P.; Zoccola, M.; Patrucco, A.; Montarsolo, A.; Rovero, G.; Tonin, C. Comparative Study on the Effects of Superheated Water and High Temperature Alkaline Hydrolysis on Wool Keratin. *Text. Res. J.* **2017**, *87* (14), 1696−1705.
(31) Aluigi, A.; Vineis, C.; Tonin, C.; Tonetti, C.; Varesano, A.; Mazzuchetti, G. Wool Keratin-Based Nanofibres for Active Filtration of Air and Water. *J. Biobased Mater. Bioenergy* **2009**, *3* (3), 311−319.
(32) Ito, K. Novel Cross-Linking Concept of Polymer Network: Synthesis, Structure, and Properties of Slide-Ring Gels with Freely Movable Junctions. *Polym. J.* **2007**, *39* (6), 489−499.
(33) Chen, J.; Garcia, E. S.; Zimmerman, S. C. Intramolecularly Cross-Linked Polymers: From Structure to Function with Applications as Artificial Antibodies and Artificial Enzymes. *Am. Chem. Soc.* **2020**, *53*, 1244−1256.
(34) Trotta, F.; Zanetti, M.; Cavalli, R. Cyclodextrin-Based Nanosponges as Drug Carriers. *Beilstein J. Org. Chem.* **2012**, *8*, 2091−2099.
(35) Hoti, G.; Caldera, F.; Cecone, C.; Rubin Pedrazzo, A.; Anceschi, A.; Appleton, S. L.; Monfared, Y. K.; Trotta, F. Effect of the Cross-Linking Density on the Swelling and Rheological Behavior of Ester-Bridged β-Cyclodextrin Nanosponges. *Materials (Basel).* **2021**, *14* (3), 1−20.
(36) Revellame, E. D.; Fortela, D. L.; Sharp, W.; Hernandez, R.; Zappi, M. E. Adsorption Kinetic Modeling Using Pseudo-First Order and Pseudo-Second Order Rate Laws: A Review. *Clean. Eng. Technol.* **2020**, *1*, No. 100032.
(37) Anceschi, A.; Zoccola, M.; Mossotti, R.; Bhavsar, P.; Dalla Fontana, G.; Patrucco, A. Colorimetric Quantification of Virgin and Recycled Cashmere Fibers: Equilibrium, Kinetic, and Thermodynamic Studies. *J. Nat. Fibers* **2022**, *19* (15), 11064−11077.
(38) Kaschuk, J. J.; Borghei, M.; Solin, K.; Tripathi, A.; Khakalo, A.; Leite, F. A. S.; Branco, A.; De Sousa, M. C. A.; Frollini, E.; Rojas, O. J. Cross-Linked and Surface-Modi Fied Cellulose Acetate as a Cover Layer for Paper-Based Electrochromic Devices. *Appl. Polym. Mater.* **2021**, *3*, 2393−2401.
(39) Song, K.; Xu, H.; Mu, B.; Xie, K.; Yang, Y. Non-Toxic and Clean Crosslinking System for Protein Materials: Effect of Extenders on Crosslinking Performance. *J. Clean. Prod.* **2017**, *150*, 214−223.
(40) Foggia, M.; Taddei, P.; Torreggiani, A.; Dettin, M.; Tinti, A. Self-Assembling Peptides for Biomedical Applications: IR and Raman Spectroscopies for the Study of Secondary Structure. *Proteomics Res. J.* **2012**, *2*, 231−272.
(41) Anceschi, A.; Caldera, F.; Bertasa, M.; Cecone, C.; Trotta, F.; Bracco, P.; Zanetti, M.; Malandrino, M.; Mallon, P. E.; Scalarone, D. New Poly(β-Cyclodextrin)/Poly(Vinyl Alcohol) Electrospun Sub-Micrometric Fibers and Their Potential Application for Wastewater Treatments. *Nanomater. (Basel, Switzerland)* **2020**, *10* (3). 482.
(42) Nandi, S.; Winter, H. H. Swelling Behavior of Partially Cross-Linked Polymers: A Ternary System. *Macromolecules* **2005**, *38* (10), 4447−4455.
(43) Hernandez-Martínez, A. R.; Lujan-Montelongo, J. A.; Silva-Cuevas, C.; Mota-Morales, J. D.; Cortez-Valadez, M. Ruiz-Baltazar, A. de J.; Cruz, M.; Herrera-Ordonez, J. Swelling and Methylene Blue

https://doi.org/10.1021/acsomega.3c09133
ACS Omega 2024, 9, 43319−43330

Adsorption of Poly (N, N -Dimethylacrylamide- Co-2-Hydroxyethyl Methacrylate) Hydrogel. *React. Funct. Polym.* **2018**, *122* (November 2017)), 75−84.
(44) Rajasulochana, P.; Preethy, V. Comparison on Efficiency of Various Techniques in Treatment of Waste and Sewage Water − A Comprehensive Review. *Resour. Technol.* **2016**, *2* (4), 175−184.
(45) Doğan, M.; Alkan, M.; Türkyilmaz, A.; Özdemir, Y. Kinetics and Mechanism of Removal of Methylene Blue by Adsorption onto Perlite. *J. Hazard. Mater.* **2004**, *109* (1), 141−148.
(46) Karnib, M.; Kabbani, A.; Holail, H.; Olama, Z. Heavy Metals Removal Using Activated Carbon, Silica and Silica Activated Carbon Composite. *Energy Procedia* **2014**, *50*, 113−120.
(47) Ibrahim, H.; Sazali, N.; Salleh, W. N. W.; Ngadiman, N. H. A.; Fadil, N. A.; Harun, Z. Outlook on the Carbon-Based Materials for Heavy Metal Removal. *Biointerface Res. Appl. Chem.* **2022**, *12* (4), 5303−5323.
(48) Ngah, W. S. W.; Fatinathan, S. Adsorption of Cu(II) Ions in Aqueous Solution Using Chitosan Beads, Chitosan−GLA Beads and Chitosan−Alginate Beads. *Chem. Eng. J.* **2008**, *143* (1), 62−72.
(49) Zia, Q.; Tabassum, M.; Gong, R.; Li, J. A Review on Chitosan for the Removal of Heavy Metals Ions. *J. Fiber Bioeng. Informatics* **2019**, *12*, 103−128.
(50) Zhang, T.; Wang, W.; Zhao, Y.; Bai, H.; Wen, T.; Kang, S.; Song, G.; Song, S.; Komarneni, S. Removal of Heavy Metals and Dyes by Clay-Based Adsorbents: From Natural Clays to 1D and 2D Nano-Composites. *Chem. Eng. J.* **2021**, *420*, No. 127574.
(51) Velarde, L.; Nabavi, M. S.; Escalera, E.; Antti, M.-L.; Akhtar, F. Adsorption of Heavy Metals on Natural Zeolites: A Review. *Chemosphere* **2023**, *328*, No. 138508.
(52) Hua, M.; Zhang, S.; Pan, B.; Zhang, W.; Lv, L.; Zhang, Q. Heavy Metal Removal from Water/Wastewater by Nanosized Metal Oxides: A Review. *J. Hazard. Mater.* **2012**, *211−212*, 317−331.
(53) Liosis, C.; Papadopoulou, A.; Karvelas, E.; Karakasidis, T. E.; Sarris, I. E. Heavy Metal Adsorption Using Magnetic Nanoparticles for Water Purification: A Critical Review. *Mater. (Basel, Switzerland)* **2021**, *14* (24). 7500.
(54) Syeda, S. E. Z.; Nowacka, D.; Khan, M. S.; Skwierawska, A. M. Recent Advancements in Cyclodextrin-Based Adsorbents for the Removal of Hazardous Pollutants from Waters. *Polymers (Basel).* **2022**, *14* (12). 2341.
(55) Aluigi, A.; Zoccola, M.; Vineis, C.; Tonin, C.; Ferrero, F.; Canetti, M. Study on the Structure and Properties of Wool Keratin Regenerated from Formic Acid. *Int. J. Biol. Macromol.* **2007**, *41* (3), 266−273.
(56) Kar, P.; Misra, M. Use of Keratin Fiber for Separation of Heavy Metals from Water. *J. Chem. Technol. Biotechnol.* **2004**, *79*, 1313−1319.
(57) Khosa, M. A.; Ullah, A. In-Situ Modification, Regeneration, and Application of Keratin Biopolymer for Arsenic Removal. *J. Hazard. Mater.* **2014**, *278*, 360−371.
(58) de la Rosa, G.; Reynel, H.; Bonilla-Petriciolet, A.; Cano-Rodriguez, I.; Velasco-Santos, C.; Martínez-Hernández, A. *Recycling Poultry Feathers for Pb Removal from Wastewater: Kinetic and Equilibrium Studies*; 2008; Vol. *30*.
(59) Aguayo-Villarreal, I. A.; Bonilla-Petriciolet, A.; Hernández-Montoya, V.; Montes-Morán, M.; Reynel, H. Batch and Column Studies of Zn2+ Removal from Aqueous Solution Using Chicken Feathers as Sorbents. *Chem. Eng. J.* **2011**, *167*, 67−76.
(60) Sun, P.; Liu, Z.-T.; Liu, Z.-W. Chemically Modified Chicken Feather as Sorbent for Removing Toxic Chromium(VI) Ions. *Ind. Eng. Chem. Res.* **2009**, *48* (14), 6882−6889.
(61) Khosa, M. A.; Wu, J.; Ullah, A. Chemical Modification{,} Characterization{,} and Application of Chicken Feathers as Novel Biosorbents. *RSC Adv.* **2013**, *3* (43), 20800−20810.
(62) Wang, S.; Wei, M.; Huang, Y. Biosorption of Multifold Toxic Heavy Metal Ions from Aqueous Water onto Food Residue Eggshell Membrane Functionalized with Ammonium Thioglycolate. *J. Agric. Food Chem.* **2013**, *61* (21), 4988−4996.
(63) Sekimoto, Y.; Okiharu, T.; Nakajima, H.; Fujii, T.; Shirai, K.; Moriwaki, H. Removal of Pb(II) from Water Using Keratin Colloidal Solution Obtained from Wool. *Environ. Sci. Pollut. Res. Int.* **2013**, *20* (9), 6531−6538.
(64) Tonetti, C.; Aluigi, A.; Selmin, F.; Cilurzo, F.; Mazzuchetti, G. Removal of Cu(II) Ions from Water Using Thermally-Treated Horn−Hoof Powder as Biosorbent. *Desalin. Water Treat.* **2014**, *55*, 1−11.
(65) Donner, M. W.; Arshad, M.; Ullah, A.; Siddique, T. Unravelled Keratin-Derived Biopolymers as Novel Biosorbents for the Simultaneous Removal of Multiple Trace Metals from Industrial Wastewater. *Sci. Total Environ.* **2019**, *647*, 1539−1546.
(66) Zubair, M.; Zahara, I.; Roopesh, M. S.; Ullah, A. Chemically Cross-Linked Keratin and Nanochitosan Based Sorbents for Heavy Metals Remediation. *Int. J. Biol. Macromol.* **2023**, *241*, No. 124446.
(67) Peiravi-Rivash, O.; Mashreghi, M.; Baigenzhenov, O.; Hosseini-Bandegharaei, A. Producing Bacterial Nano-Cellulose and Keratin from Wastes to Synthesize Keratin/Cellulose Nanobiocomposite for Removal of Dyes and Heavy Metal Ions from Waters and Wastewaters. *Colloids Surfaces A Physicochem. Eng. Asp.* **2023**, *656*, No. 130355.

https://doi.org/10.1021/acsomega.3c09133
ACS Omega 2024, 9, 43319−43330

A novel approach for nanosponge: wool waste as building block for the synthesis of keratin based nanosponge and perspective application in wastewater treatment

Gjylije Hoti[1,2], Fabrizio Caldera[1], Francesco Trotta[1], Marina Zoccola[3], Alessia Patrucco[3], Anastasia Anceschi*[3]

[1] *Department of Chemistry, University of Turin, Via P. Giuria 7, 10125 Turin, Italy*
[2] *Department of Drug Science and Technology, University of Turin, Via P. Giuria 9, 10125 Turin, Italy (Current Affiliation)*
[3] *CNR-STIIMA, Italian National Research Council, Institute of Intelligent Industrial Technologies and Systems for Advanced Manufacturing, Corso G. Pella 16, 13900, Biella (BI), Italy.*

**Corrisponding Author: anastasia.anceschi@stiima.cnr.it*

Supporting Information (SI)

In Figure S1, a section of the IR spectrum is presented for keratin, keratin-based nanosponge (Ker-NS), and the physical mixture of keratin and pyromellitic dianhydride (PMDA). The spectrum highlights key differences between the chemically cross-linked Ker-NS and the physical mixture, providing insights into the nature of the cross-linking reaction.

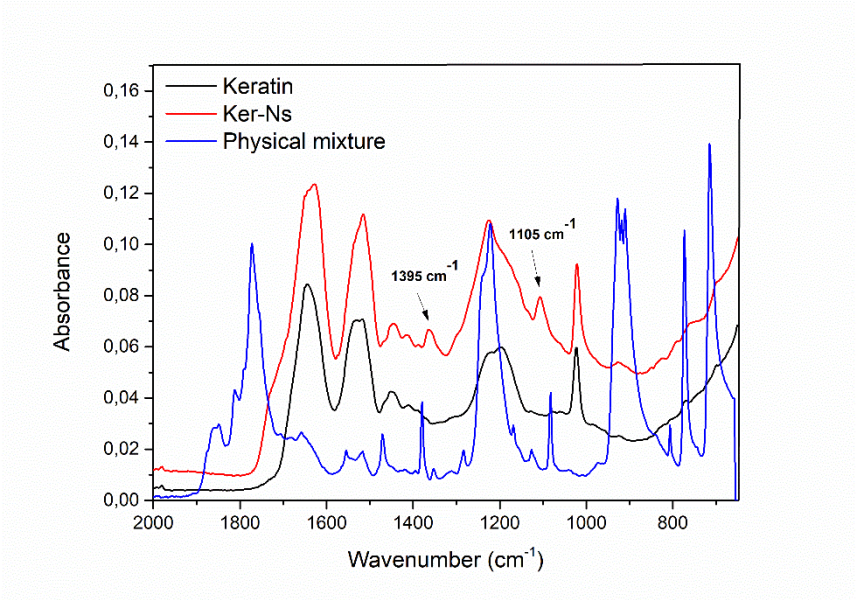

Figure S1: FTIR spectra of Keratin, Ker-Ns and the physical mixture

The IR spectrum of Ker-NS exhibits two distinct peaks at 1395 cm^{-1} and 1105 cm^{-1}, which are absent in the spectrum of the physical mixture. These peaks are associated with the cross-linking between keratin and PMDA. In particular, the peak at 1395 cm^{-1} corresponds to the O-H bending vibration of the carboxyl group, which is indicative of ester or anhydride linkage formation in the cross-linked polymer, whereas the peak at 1105 cm^{-1} is attributed to C-O stretching vibrations, further confirming the formation of ester bonds as a result of the cross-linking process. The absence of these peaks in the physical mixture indicates that they arise specifically from the chemical reaction between keratin and PMDA, rather than from simple physical blending. This underscores the successful formation of

covalent bonds during the cross-linking process. This confirms the transformation of functional groups into a stable, cross-linked network. The IR spectral analysis thus corroborates the successful chemical modification of keratin through cross-linking with PMDA, which is pivotal to the performance characteristics of the keratin-based nanosponge.

For better understand the cross-linking reaction, also the DSC of the physical mixture has been performed. As shown in figure S2, in the DSC analysis of the physical mixture of keratin and PMDA, no peaks are observed in the temperature range between 160°C and 180°C, in contrast to the distinct peak seen in the DSC of Ker-Ns (see Figure 4).

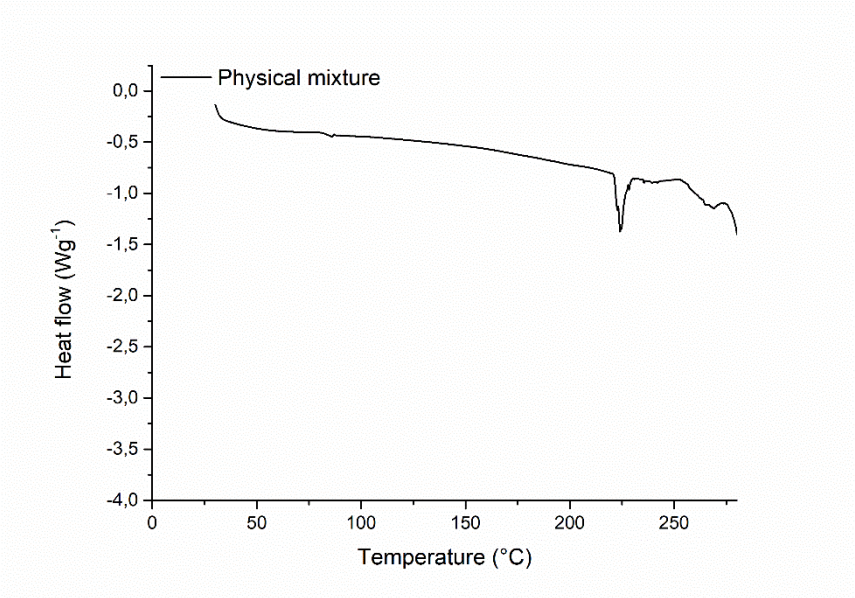

Figure S2: DSC of the physical mixture

The physical mixture of keratin and PMDA lacks a chemical reaction between the components. As a result, there are no thermal events related to the formation of new chemical bonds, which would manifest as distinct peaks in the DSC thermogram. The mixture remains a simple blend of the two materials without any interaction at the molecular level. In the Ker-Ns, a chemical reaction occurs between keratin and PMDA, leading to the formation of a cross-linked polymer network. This reaction introduces new chemical bonds, such as ester linkages, which are responsible for the thermal transitions observed in the DSC at 160°C to 180°C. The presence of a distinct thermal event in the Ker-Ns and its absence in the physical mixture corroborates the occurrence of cross-linking, which fundamentally alters the material's thermal behavior. This change enhances the thermal stability and mechanical properties of Ker-Ns, making it more suitable for practical applications.

In summary, the DSC analysis provides compelling evidence of the chemical modifications in Ker-NS, distinguishing it from the simple physical mixture and highlighting the role of cross-linking in enhancing material properties.

In table S1 are reported all the data used for the calculation of the amount of heavy metals adsorbed by the Ker-Ns.

Ni

Time (h)	Initial concentration (mg/L)	Quantity adsorbed (for three replicas) (mg/L)	Quantity adsorbed (%)	Standard deviation
1	50	18.40 18.54 18.32	36.84	0.20
3	50	26.31 26.13 26.54	52.62	0.21
5	50	26.97 26.83 27.07	53.94	0.12
24	50	27.43 27.35 27.4	54.8	0.01
Cd				
1	50	17.80 18.00 17.89	35.80	0.08
3	50	27.78 27.94 27.92	55.76	0.06
5	50	27.94 27.85 28.16	55.97	0.20
24	50	27.94 27.92 28.06	55.92	0.05
Pb				
1	50	18.15 18.23 18.09	36.30	0.04
3	50	26.95 27.03 27.06	54.03	0.03
5	50	26.55 26.74 26.61	53.26	0.08
24	50	27.05 27.17 27.09	54.21	0.03

Table S1: ICP results obtained for the heavy metal adsorption

Table S1 shows the quantity of each metal adsorbed (in mg/L) at multiple time points (1, 3, 5, and 24 hours) after exposure to a 50 mg/L initial concentration. Moreover, it reports the percentage of metal ions adsorbed, which doubles as a measure of the efficiency of Ker-Ns. For instance, by 24 hours, approximately 54.8% of Ni, 55.92% of Cd, and 54.21% of Pb were adsorbed, indicating high efficiency over a day-long period. The inclusion of data from three replicas for each measurement point underlines the reproducibility and reliability of the results. Standard deviations are also provided, which are crucial for assessing the precision of the measurements. The low standard deviation values, particularly evident in the 24-hour measurements across all metals, indicate the consistent performance of the Ker-Ns in these experiments. Indeed, the observed decrease in standard deviations over time suggests the possibility of stabilization of the adsorption process as the system approaches equilibrium.